THE JOURNAL OF GENE MEDICINE
J Gene Med 2015; **17**: 116–131.
Published online in Wiley Online Library (wileyonlinelibrary.com) **DOI:** 10.1002/jgm.2830

RESEARCH ARTICLE

Effective multiple oral administration of reverse genetics engineered infectious bursal disease virus in mice in the presence of neutralizing antibodies

Ákos Hornyák[1]
Kai S. Lipinski[2]
Tamás Bakonyi[3]
Petra Forgách[3]
Ernő Horváth[1]
Attila Farsang[1]
Susan J. Hedley[4,8]
Vilmos Palya[5]
Tibor Bakács[6]
Imre Kovesdi[6,7]*

[1]*National Food Chain Safety Office, Budapest, Hungary*

[2]*Vibalogics GmbH, Cuxhaven, Germany*

[3]*Department of Microbiology and Infectious Diseases, Faculty of Veterinary Science, Szent István University, Budapest, Hungary*

[4]*VectorLogics, Inc., Birmingham, AL, USA*

[5]*CEVA-Phylaxia Inc., Budapest, Hungary*

[6]*HepC Ltd, Budapest, Hungary*

[7]*ImiGene, Inc., Rockville, MD, USA*

[8]*Present address: Meridian Life Science, Inc., Memphis, TN, USA*

*Correspondence to:
I. Kovesdi, ImiGene, Inc., 7713 Warbler Ln, Rockville, MD 20855, USA.
E-mail: ikovesdi@imigeneinc. com

Received: 4 December 2014
Revised: 21 March 2015
Accepted: 24 April 2015

Abstract

Background Despite spectacular successes in hepatitis B and C therapies, severe hepatic impairment is still a major treatment problem. The clinically tested infectious bursal disease virus (IBDV) superinfection therapy promises an innovative, interferon-free solution to this great unmet need, provided that a consistent manufacturing process preventing mutations or reversions to virulent strains is obtained.

Methods To address safety concerns, a tissue culture adapted IBDV vaccine strain V903/78 was cloned into cDNA plasmids ensuring reproducible production of a reverse engineered virus R903/78. The therapeutic drug candidate was characterized by immunocytochemistry assay, virus particle determination and immunoblot analysis. The biodistribution and potential immunogenicity of the IBDV agent was determined in mice, which is not a natural host of this virus, by quantitative detection of IBDV RNA by a quantitative reverse transcriptase-polymerase chain reaction and virus neutralization test, respectively.

Results Several human cell lines supported IBDV propagation in the absence of visible cytopathic effect. The virus was stable from pH 8 to pH 6 and demonstrated significant resistance to low pH and also proved to be highly resistant to high temperatures. No pathological effects were observed in mice. Single and multiple oral administration of IBDV elicited antibodies with neutralizing activities *in vitro*.

Conclusions Repeat oral administration of R903/78 was successful despite the presence of neutralizing antibodies. Single oral and intravenous administration indicated that IBDV does not replicate in mammalian liver alleviating some safety related concerns. These data supports the development of an orally delivered anti-hepatitis B virus/ anti-hepatitis C virus viral agent for human use. Copyright © 2015 John Wiley & Sons, Ltd.

Keywords IBDV; immune response; infectious bursal disease virus; oral dosing; replication; superinfection therapy

Introduction

Infectious bursal disease virus (IBDV) belongs to the genus *Avibirnavirus* and is a member of the family *Birnaviridae*. It is the causative agent of a highly

immunosuppressive disease in young chickens [1]. Infectious bursal disease (IBD) or Gumboro disease is characterized by the destruction of lymphoid follicles in the bursa of Fabricius. Because of its major economic importance to the world's poultry industries, attenuated IBDV strains are used as commercial vaccines, and some of them are propagated in Vero cells. These vaccines have an excellent safety record [2]. IBDV is not known to be a hazard with respect to transmission to other species despite its worldwide distribution in the domestic fowl [1,3].

The genome of IBDV consists of two segments of double-stranded (ds)RNA that are packaged in a nonenveloped icosahedral shell of 60 nm in diameter [4]. The capsid of the IBDV virion consists of several structural proteins. The larger segment A is 3261 nucleotides long for the vaccine strain D78 [5] and it encodes a 110-kDa precursor protein in a single large open reading frame (ORF), which is cleaved by viral protease, VP4, to yield mature VP2, VP3 and VP4 proteins. In addition, segment A encodes a 17-kDa nonstructural protein, also known as VP5, from a small ORF partly preceding and overlapping the polyprotein ORF. VP2 is the major host-protective immunogen of IBDV. The smaller segment B is 2827 nucleotides long, and it encodes VP1, a 97-kDa protein with RNA-dependent RNA polymerase activity [6,7]. IBDV infects the precursors of antibody-producing B cells in the bursa of Fabricius. Studies have shown that virulent strains of IBDV lose their virulent potential after serial passage in non-B lymphoid chicken cells. Comparison of the deduced amino acid sequences of the virulent and attenuated strains show specific amino acid substitution within the hypervariable region of the VP2 protein [8].

Procedures developed during the 1990s to genetically manipulate the genomes of negative-strand RNA viruses and to rescue infectious viruses entirely from cloned cDNAs, commonly referred to as reverse genetics, have revolutionized the analyses of viral gene expression, viral replication and pathogenesis. They have also paved the road for the engineering of these viruses for vaccine and gene therapy development [9]. It has been also shown that segmented dsRNA virus, such as IBDV, can be recovered from cloned-derived transcripts of its genomic segments A and B [10–12].

Over a decade ago, clinical trials were set up to use a conventionally produced IBDV as a therapeutic agent with patients suffering from acute and chronic hepatitis C virus (HCV) and hepatitis B virus (HBV) infections [13,14]. IBDV was chosen because of the nonpathological profile in humans and no toxicity was seen in these patients. The strategy behind these clinical trials was to exploit viral competition for the treatment of persistent viral infections. This idea is based on the clinical observation that unrelated viruses might interact in co-infected patients. Hepatitis infection by one type of virus is often abolished after accidental infection by a second hepatitis virus [15,16]. Apparently, replication of two different viruses may interact in co-infected patients such that the dominant virus terminates the replication of the other virus [17–19]. Nevertheless, in cases when both viruses are pathogenic, the disease persists and hepatitis remains. However, the patient may benefit from superinfection with a nonpathogenic dsRNA virus such as IBDV [20]. Our unpublished preclinical data indicates that R903/78 is a potent activator of the interferon-dependent innate antiviral gene program, which could explain its strong interference with unrelated viruses. Therefore, it is not essential for IBDV to infect the same cells that are infected by HCV or HBV *in vivo* as the interference is probably mediated through secreted cytokines. In such a way, and with the aim of resolving persistent HBV or HCV infections, viral competition can be exploited by a nonpathogenic, attenuated vaccine strain of IBDV.

The results of a phase II clinical trial of IBDV superinfection therapy in 42 acute hepatitis patients showed the safety and efficacy of IBDV therapy [21]. Despite being an extensively used vaccine, information about its physical characteristics remains scarce [22,23]. The use of IBDV as an agent against a human disease requires a well characterized drug candidate. Therefore, in the present study, we have cloned the V903/78 vaccine strain and assembled it into cDNA plasmids allowing reproducible viral production. Phylogenic relations to other IBDV strains placed this virus within the tissue adapted vaccine strains with the closest relationship to D78. We have also thoroughly characterized this therapeutic drug candidate by determining its temperature and pH resistance, as well as by evaluating its immunogenicity, biodistribution and replicating potential in mice after single and multiple dosing.

Materials and methods

Cell lines used

Vero (African green monkey, kidney), HepG2 (human hepatocellular carcinoma, liver), HEK293 (human, kidney), A549 (human carcinoma, lung), U937 (human, histiocytic lymphoma, monocyte) and THP1 (human acute monocytic leukemia, monocyte) cells were purchased from ATCC (Manassas, VA, USA). All cell lines were maintained as advised by the ATCC.

Sequencing of the V903/78 virus

The viral RNA was extracted and purified from Vero cells as described previously [4]. Briefly, sodium dodecyl

DOI: 10.1002/jgm

sulfate (final concentration, 2% w/v) and proteinase K (final concentration, 250 μg/μl) was added to the infected cell culture and the mixture was incubated for 5 min at 55 °C. Viral RNA was extracted with acid phenol: chloroform (5:1, pH 4.7) (Ambion/Life Technologies, Carlsbad, CA, USA) and chloroform:isoamyl alcohol (49:1) and further purified using the RNaid kit (BIO101, Carlsbad, CA, USA). Finally, the RNA was resuspended in diethylpyrocarbonate (DEPC) treated water and stored at –80 °C until used in the reverse transcriptase (RT) reaction, which was performed as described previously [4]. Denaturation of the dsRNA was performed by boiling the samples for 5 min and rapid chilling to 0 °C before the reverse transcription. Next, 5 μl denatured RNA was used as template for the reverse transcription using Moloney murine leukemia virus (MMLV)-reverse transcriptase and random hexamer primers. The reaction was made using the mixture: 5 μl of 5 × RT buffer, 4 μl of 2.5 mM dNTP, 1 μl of 50 μg/ml random hexamer, 40 U of RNase inhibitor, 200 U of MMLV enzyme and DEPC-treated water to a final volume of 25 μl. The reaction mixture was incubated for 1.5 h at 37 °C. The polymerase chain reaction (PCR) reaction mixture contained: 5 μl of 10 × PCR buffer, 5 μl of 25 mM $MgCl_2$, 0.5 μl of 10 mg/ml bovine serum albumin (BSA), 1.5 μl of 2.5 mM dNTP, 1.0 μl of 10 μM of each primer, 0.4 μl of 5 U/μl Taq polymerase and water to a 50-μl final reaction volume. Overlapping primers were used to amplify genomic segments A and B of V903/78 IBDV strain. Primers used for segment A were: 1-GGATACGATCGGTCTGA; 2-CCTTGGACGCTTGTTTG; 3-GTGGGGTAACAATCACACTG; 4-TGTGCACCGCGGAGTA; 5-TACGAGGTAGTCGCGAATCT; 6-GACTTGCTGCCTGCTTGT; 7-TGTGGCTGGAAGAGAATG; 8-AGGGGACCCGCGAAC. Primers used for segment B were: 1-GGATACGATGGGTCTGAC; 4-CAATTGAGTACCACGTGTT; 5-TAACCTGGCCCGTGATGTCC; 6-CCTACCAACCTCAACGC CTC; 7-ACAGCCAGGGTACCTGAGTG; 8-GGGGGCCCCCGC AGG. After denaturing the template DNA for 2 min at 94 °C, amplification consisted of 30 cycles of denaturation (30 s at 94 °C), primer annealing (30 s at 55 °C) and primer extension (1 min at 72 °C) with a single extension step of 10 min at 72 °C. The results of the PCR products were visualized on 1.5% agarose gels with ethidium bromide staining and these were purified using a QIAquick PCR purification kit (Qiagen, Hilden, Germany). The purified PCR products were sequenced in both directions using a BigDye Terminator Cycle sequencing kit (Applied Biosystems/Life Technologies, Carlsbad, CA, USA) in accordance with the manufacturer's instructions.

Sequencing of the reverse genetically created R903/78 virus

Sequencing of the reverse engineered R903/78 viruses were performed in accordance with methods described by Costa *et al.* [24] using overlapping primers for both segments. The 5'- and 3'-ends of the segments were also sequenced by rapid amplification of cDNA ends (RACE) with the appropriate primers.

For determination of the 5'- and 3'-ends of the segments, the viral RNA was extracted and purified from Vero cells with QIAamp Viral RNA Mini kit (Qiagen), as well as the MagMAX Viral RNA Isolation Kit (Ambion). Viral RNA was used as template for RT-PCR using the OmniScript RT kit from Qiagen. RT-PCR, poly (A) tailing and cDNA synthesis was performed according to Ammayappan *et al.* [25]. Reactions were carried out in accordance with the manufacturer's instructions. To identify the 3'-terminal region of the genomic RNA, poly (A) tail was added to the 3'-end with poly (A) polymerase enzyme in accordance with the manufacturer's instructions (Applied Biosystems). The tailing reaction was carried out in a tube containing 30 μl of RNA, 26 μl of nuclease free water, 20 μl of 5 × poly (A) polymerase buffer, 10 μl of 25 mM $MnCl_2$, 10 μl of 10 mM ATP and 4 μl of *Escherichia coli* poly (A) polymerase. The reaction mixture was incubated at 37 °C for 1 h and then RNA was purified using a Qiagen RNAeasy kit in accordance with the manufacturer's instructions. The cDNA synthesis and polymerase chain reaction were conducted as described above, using an oligo (dT) primer (5'-GCGGCCGCTTTTTTTTTTTTTTTTTTTT-3') for the first-strand synthesis, followed by PCR with the IBDV specific primers. The 5'-terminal of genomic RNA was identified by rapid amplification of the 5'-end, using a 5' RACE kit (Invitrogen/Life Technologies, Carlsbad, CA, USA) in accordance with the manufacturer's instructions. Internal sequences were amplified with RT-PCR as described above and sequenced.

The complete nucleotide sequence of the reverse genetically created R903/78 virus was assembled and was found to be identical to the parental V903/78 virus sequence previously reported and published in GenBank. The nucleotide sequence of IBDV V903/78 was deposited in GenBank. Segment A is available under accession number JQ411012 and segment B under accession number JQ411013.

Phylogenetic tree analysis

Sequences of V903/78 and sequences of the relevant IBDV strains obtained from the GenBank database were aligned by ClustalW multiple alignment method using the Bioedit sequence alignment editor (http://www.mbio.ncsu.edu/BioEdit/bioedit.html). Sequence differences were calculated by Kimura's two-parameter method. A phylogenetic tree was constructed using the neighbor-joining method with TREECON [26]. Australian

IBDV strain 000273/AU was used as the outgroup. Bootstrap analysis was performed using 1000 bootstrap samples with TREECON.

Virus propagation

Viruses were propagated in Vero cells essentially as described by Kibenge *et al*. [1]. Vero cells (ATCC) were grown to complete confluency in Dulbecco's modified Eagle's medium (DMEM) (Life Technologies) containing 5% serum and antibiotics. Cells were infected with virus stocks at a multiplicity of infection (MOI) of 0.1–0.2 infectious units (IU)/cell and grown in DMEM containing 2% serum and incubated at 37 °C in a CO_2 incubator. Virus stocks were prepared as clarified lysates (10 000 ***g*** for 15 min at 4 °C) and harvested at day 4 post-infection (PI). Viral supernatants were stored at –80 °C. Apparently, this virus strain did not produce a cytopathic effect (CPE) on Vero cells and the great majority of virus (approximately 90%) was detected in the supernatant at 4 days PI by virus titration. Therefore, there was no need to disrupt the cells.

Virus titration using immunocytochemistry assay (ICC) and virus particle determination

Infectious virus titer (IU) was determined by the ICC assay in 24-well plates. Monolayers of Vero cells were infected with serial dilutions of the virus. After incubation for approximately 24 h, the viral solution was aspirated and cells were fixed in cold 90% methanol for 10 min at room temperature. Wells were washed with Ca^{2+}- and Mg^{2+}-free phosphate-buffered saline (PBS)/1% BSA and then probed with a chicken anti-IBDV antibody (Charles River Laboratories, Wilmington, MA, USA) in PBS/1% BSA for 60 min (1:600 dilution; 250 µl/well). The primary antibody was removed, plates were washed again three times and cells probed with a secondary rabbit anti-IgY peroxidase antibody (Sigma-Aldrich, St Louis, MO, USA) in PBS/1% BSA for 35 min (1:1000 dilution; 250 µl/well). Plates were washed and then Trueblue solution (KPL, Gaithersburg, MD, USA) was added (250 µl/well) and incubated for 10 min. Trueblue solution was then removed and cells were washed once with dH_2O and air dried. To determine the infectious titer, the stained and infected cells were counted. Digital photos were taken from each well of the stained 24-well plates using an Eclipse TS100 microscope in conjunction with NIS Elements software (Nikon, Tokyo, Japan). Digital images were subsequently printed for counting. Titer was calculated on the basis of the number of stained cells per field (an average of 10 fields was counted) and the optical properties of the microscope were taken into account.

For determination of the total particle titer (VP) virus solutions were analysed with NanoSight NS300 equipment (Malvern Instruments, Malvern, Worcestershire, UK). The total particle number and active titer ratio (VP/IU) was in the approximate range 500–1000 for different IBDV productions.

Immunoblot analysis of IBDV proteins

Vero cells were co-transfected with pIBDV segment A and pIBDV segment B. At 5 days post-transfection, virus was harvested by three cycles of freeze–thaw. The lysed proteins were separated on 12.5% sodiun dodecylsulfate-polyacrylamide gel electrophoresis (SDS-PAGE), blotted onto nitrocellulose and reacted with polyclonal anti-IBDV rabbit serum P2D78 (a gift from Dr Vikram Vakharia, UMBC, Baltimore, MD, USA).

Evaluation of thermostability

For accelerated thermostability evaluation, the R903/78 virus was diluted into PBS and incubated at 22 °C and 48 °C for 0, 5, 15, 30, 60, 120 and 240 min. The '0' point was quick frozen on dry ice before the start of incubations. At the time points, 100-µl aliquots of virus were pipetted into 1.9 ml of pre-cooled PBS, vortexed and then quick frozen on dry ice. The tubes were stored at –80 °C until assayed for virus infectivity using the ICC assay.

For long-term thermostability evaluation, the bulk harvest was purified using depth filtration (SUPRAcap50 PDH4; Pall Corp, Port Washington, NY, USA) and concentrated with a Sartoflow Slice 200 bench top system (Sartorius, Gottingen, Germany) with a 300-kDa molecular weight cut-off polyethersulfone ultrafiltration cassette. Subsequently, the concentrated virus suspension was washed with five discontinuous diafiltration steps in the same unit and formulated into 10 mM Tris base, pH 7.8, at room temperature, 75 mM NaCl, 1 mM $MgCl_2$, 0.0025% polysorbate 80 containing (A) 15% (w/v) sucrose or (B) 10% (w/v) sucrose and 5% (w/v) trehalose. After washing a filtration step with a pore size of 0.2 µm (Pall Supor EKV) was performed to sterilize the final-formulated drug substance.

Evaluation of pH stability

Virus was diluted 1:20 into pH 2.0, 3.0, 4.0, 6.0, 7.0, 8.0 and 10.0 buffered saline solutions (VWR, Radnor, PA, USA). The virus was incubated at 37 °C for 60 min and, at the end of incubation, 200 µl of virus was immediately

DOI: 10.1002/jgm

pipetted into labeled microcentrifuge tubes containing 800 μl of Opti-MEM media (Life Technologies) and quick frozen on dry ice (1:5 dilution). The tubes were stored at –80 °C until assayed for virus infectivity with the ICC assay in accordance with the ICC protocol.

Single-step growth kinetics

Single-step growth kinetics were performed according to Kibenge *et al.* [1]. Cells were grown in 24-well plates at 37 °C in a humidified 5% CO_2-in-air atmosphere to 80–100% confluence. Virus stocks V903/78 (titer = 1.0×10^8 IU/ml) and R903/78 (titer = 8.5×10^6 IU/ml) were appropriately diluted to achieve an MOI = 0.2 IU/cell in 200 μl of medium without fetal bovine serum in duplicate. After a 2-h incubation at 37 °C, cell monolayers were washed once with warm PBS to reduce residual seed virus levels and 0.5 ml of DMEM with 5% fetal calf serum (FCS) was added and incubated at 37 °C in 5% CO_2 (suspension cells were gently spun down and re-suspended in media). At intervals after infection (relative to the end of the adsorption period), at 12, 24, 48, 72 and 96 h, supernatants from the appropriate wells were transferred to labeled tubes, briefly centrifuged and frozen at –80 °C. The tubes were stored at –80 °C until assayed for virus infectivity using the ICC assay.

Animals and immunizations

Six- to 8-week-old female and male Balb/C mice were purchased from Charles River Laboratories. Upon arrival, the mice were placed in quarantine for 7 days. Each mouse was examined closely during the quarantine period for health status. Each mouse was allowed *ad libitum* access to certified rodent diet and drinking water during the quarantine and study periods.

Mice ($n = 56$) were randomized into four groups. Group 1 ($n = 4$) comprised non-infected control, group 2 ($n = 16$) was single oral administration (SO) on day 0, group 3 ($n = 16$) was injected intravenously (IV) on day 0, and group 4 ($n = 20$) was multiple oral administrations (MO) five times on days 0, 3, 7, 13 and 20. Mice in three groups (SO, IV and MO) were administered 50-μl aliquots of 1.7×10^6 IU virus. Blood was taken for neutralization assays and necropsy performed for biodistribution on day 21 for group 1 ($n = 4$), on days 4, 8, 14 and 21 for groups 2 and 3 ($n = 4$ at each time point) and on days 1, 4, 8, 14 and 21 for group 4 ($n = 4$ at each time point). All mouse studies were carried out under a protocol approved by the Institutional Animal Care and Use Committees (Permission no. 33/2013).

Virus neutralization test (VNT)

VNT was carried out in flat-bottom 96-well micro titer plates. Vero cells were seeded at approximately 1.0×10^4 cells per well in 100 μl of DMEM + 5% FCS. Cells were incubated overnight at 37 °C in a humidified 5% CO_2-in-air atmosphere until they reached approximately 80–100% confluence on the next day. Serum samples were inactivated for 30 min at 56 °C. Next, 2 μl of serially diluted serum was pre-incubated with 25 μl of virus solute at 37 °C for 2 h to allow neutralization of the virus. Virus was diluted by 10^4 to produce approximately 100 IU/well prior to adding any serum. Thereafter, the serum/virus mixture was transferred to the Vero cell containing plates and plates were incubated for 24 h at 37 °C under 5% CO_2. Next, a standard ICC assay, as described above, was performed and the number of blue plaques was counted. Chicken IBDV antiserum was used as a positive control (Charles River Laboratories). Data were analyzed by end-point dilution. The end-point (serum titer) is expressed as the reciprocal of the highest serum dilution that completely inhibited plaque formation.

IBDV biodistribution of multiple oral dosing in mice

Biodistribution was performed on blood, feces, liver, spleen, intestine, heart, lung, kidney and gonads using quantitative detection of IBDV RNA with a quantitative (q)RT-PCR that indicated the presence of IBDV in tissue samples. Organs were homogenised for 30 s with a Qiagen Tissuelyser Retsch homogenisator (Qiagen). Organ suspension was centrifuged at 6000 ***g*** for 5 min and viral RNA was extracted using QIAamp Viral RNA Mini Kit (Qiagen) in accordance with the manufacturer's instructions. SuperScript Platinum III one-step QRT-PCR Kit (Invitrogen) was used for qRT-PCR. IBDV_A_3031F (5'-GACTGCGATGGAGATGAAGCA-3') and IBDV_A_3092R (5'-GTTTTGGCTTGGGCTTTGGT-3') primers and probe IBDV_A_3054P (FAM-GCAATCCCAGGCGGGCTC-TAMRA) were used in a 25-μl reaction in accordance with the manufacturer's instructions. Reverse transcription at 50 °C for 15 min was followed by polymerase activation at 95 °C for 2 min and 45 cycles of denaturation at 95 °C for 15 s and annealing/extension at 60 °C for 30 s. A fluorescent signal was detected in the annealing/extension steps. All runs included positive and negative controls. The positive control comprised undiluted R903/78 sample, whereas the negative control was AVL buffer of the QIAamp Viral RNA Mini Kit. The detection limit of the assay was calculated at between approximately one and 10 genomic particles.

DOI: 10.1002/jgm

Results

The IBDV V903/78 strain is closely related to the attenuated D78 vaccine strain

Strain V903/78 of IBDV was obtained from domestic poultry in Hungary in 1978. The virus strain was isolated from the bursal tissues of a 3-week-old healthy broiler chicken by inoculation of 11-day-old embryonated specified pathogen-free (SPF) eggs. The virus grown in the embryonated eggs was adapted to Vero cell culture. After 16 passages in the cell line, the strain was plaque-purified in chicken embryo fibroblast primary culture on which it causes CPE. The stock of virus designated as V903/78 passage 19 was produced for genomic characterization. This strain does not induce disease in SPF chickens after artificial infection and therefore it was considered to be attenuated. This is supported by sequence analysis data of the VP2 gene of the V903/78 strain, which shows the closest relationship with other tissue adapted, nonvirulent vaccine strains (Figure 1). Initially, a nested PCR method was used to amplify a 414-bp product spanning from 750 to 1163 nucleotides, as numbered by Bayliss *et al*. [27], which encompasses the hypervariable region of the VP2 gene. The nucleotide and deduced amino acid sequences of the hypervariable region of the VP2 gene of strain V903/78 were determined and compared with published sequences of known IBDV strains. Based on the nucleotide and deduced amino acid sequence comparisons, strain V903/78 was shown to have a unique nucleotide and amino acid sequences, and could clearly be differentiated from other known IBDV strains. Phylogenetic analysis was performed according to Ammayappan *et al*. [25] and is presented in Figure 1. It is deduced that IBDV strain D78 is the most closely related strain to V903/78.

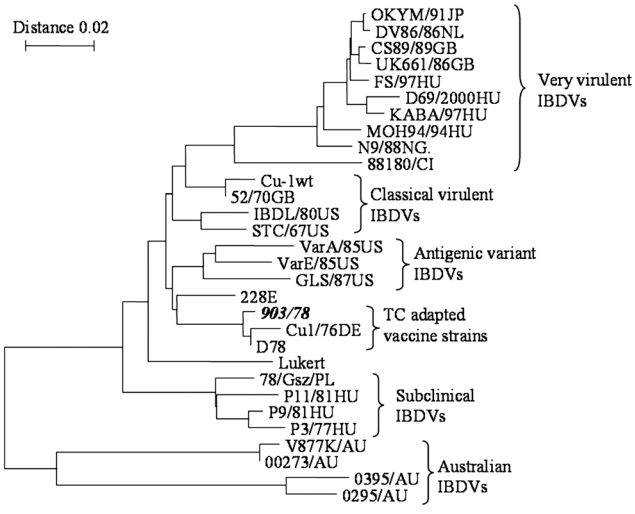

Figure 1. The phylogenetic tree of V903/78 isolate. Strain V903/78 has the closest relationship with other tissue adapted vaccine strains. IBDV vaccine strain D78 is the most closely related strain to V903/78. Phylogenetic tree analysis was conducted by neighbor-joining method using 1000 bootstrap replications. The scale indicates the number of substitution events and bootstrap confidence values are shown at branch nodes.

To compare the sequence divergence of V908/78 from the D78 strain, the entire nucleotide sequence of the V908/78 strain was sequenced as described in the Materials and methods. The nucleotide sequence of IBDV 903/78 deposited in GenBank under accession numbers JQ411012 for segment A and JQ411013 for segment B was aligned with sequences of D78 listed under accession number EU162087 [5] for segment A and EU162090 [5,28] for segment B. Comparing strain D78 with V903/78 segment A, there were eight point mutations and one deletion. Two mutations and one deletion are in the noncoding regions, which might be significant because these regions are involved in RNA polymerase binding and could significantly change the growth characteristics of the virus. Two further mutations did not result in amino acid changes and four mutations resulted in five amino acid changes. One nucleotide change resulted in two amino acid changes because VP5 and VP2 have overlapping reading frames. Therefore, there is one amino acid change in VP5 and one amino acid change in the VP4 regions. There are three amino acid changes in the VP2 protein region, although the amino acids determining cell tropism and virulence (amino acids 253H, 279 N and 284 T) are identical between D78 and V903/78 [8,29,30]. These changes are listed in Table 1. Comparing segment B, there were nine point mutations and, of the six in the coding region, none resulted in amino acid changes. These mutations are listed in Table 2.

Cloning of the V903/78 genome and recovery of the R903/78 virus

Construction of full-length cDNA clones of IBDV segments A and B of strain D78 has been described previously [10] and the clones were used as templates to generate pIBDVA (D78) and pIBDVB (D78) plasmids. The genome fragments were amplified using their respective primers, as reported in Upadhyay *et al*. [12], and the segments were fused to a cytomegalovirus (CMV) promoter transcription start site of the pCI vector (Promega, Madison, WI, USA) at their 5'-end and hepatitis delta ribozyme (HDR) sequence at their 3'-end, as described in Ben Abdeljelil *et al*. [11]. Both plasmids were sequenced to confirm the identity of segment A and segment B.

DOI: 10.1002/jgm

Table 1. Mutational analysis of segment A between IBDV strains D78 and V903/78

Location	D78 nucleotides	V903/78 nucleotides	D78 amino acids	V903/78 amino acids	Notes
54	C	T			Noncoding
69	G	A			Noncoding
102	T	C			Coding
356	G	A	G	E	VP5 amino acids 87
			G	S	VP2 amino acids 76
893	C	A	L	I	VP2 amino acids 255
938	A	G	T	A	VP2 amino acids 270
1453	A	C			Coding
2235	C	A	T	K	VP4 amino acids 190
3231	ATC	Δ			Noncoding – deletion

Table 2. Mutational analysis of segment B between IBDV strains D78 and V903/78

Location	D78 nucleotides	V903/78 nucleotides	Notes
14	C	T	Noncoding
23	T	A	Noncoding
41	G	A	Noncoding
942	A	C	Coding
1095	T	C	Coding
1158	C	T	Coding
1627	T	C	Coding
1938	G	A	Coding
2511	C	T	Coding

Mutational analysis between strains D78 and V903/78 was performed as described above. Oligonucleotide primers were designed that incorporated the V903/78 nucleotide changes and the correct PCR fragments were generated using the D78 plasmids as templates. The new V903/78 fragments were exchanged with the original D78 fragments in the expression plasmids creating pCMV-903/78-SegA and pCMV-903/78-SegB plasmids illustrated in Figure 2. To generate the new R903/78 virus, both segment A and B (1 μg of each) were transfected into Vero cells. Virus production was monitored by immunoblotting. Successful virus recovery was achieved only when both segments were co-transfected. The recovered virus was characterized by western blotting [12]. Western blot analysis of infected Vero cell lysates with anti-IBDV polyclonal antibody P2D78 (a gift from Dr Vikram Vakharia, UMBC) confirmed the presence of the recovered R903/78 virus only in the Superfect (Qiagen) but not in the Dotap (Roche, Basel, Switzerland) transfected cells (Figure 3).

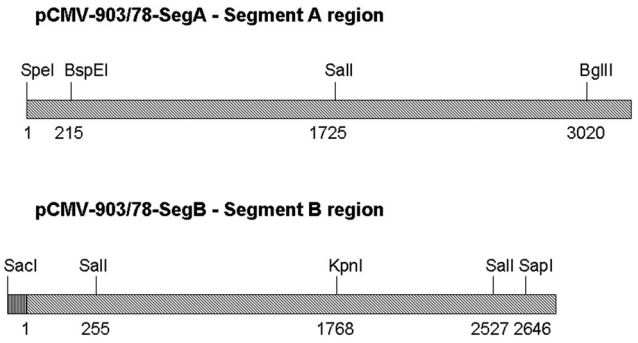

Figure 2. Construction of the IBDV R903/78 strain. Depicted are the relevant restriction sites used in the exchange of restriction fragments between D78 and R903/78. The *Sac*I site is in the CMV promoter of the expression plasmid. Numbers indicate the nucleotide positions according to Bayliss *et al*. [19].

Several virus clones were isolated and sequencing of the viruses were performed according to methods described by Costa *et al*. [24] using overlapping primers for both segments. The 5'- and 3'-ends of the segments were sequenced by RACE with specific primers (see Materials and methods).

All viruses isolated had identical sequence to the original V903/78 virus, except for one isolate, which had only four 'C' instead of five at the 3'-end of segment B. Although several comparisons of viral production did not indicate any statistical difference between the two different virus isolates, the so-called four 'C' virus was not used in any further experiments.

To determine the genetic stability of the reverse genetically engineered R903/78 virus, the virus was propagated in Vero cells (up to five passages), total RNA was isolated and a portion of VP5 gene was amplified by RT-PCR. Sequence analysis of the RT-PCR product confirmed the expected sequence of the VP5 gene of the recovered virus. The stability of the rescued virus was further confirmed by western blot analysis of the cell lysates (data not shown).

Growth kinetics of the rescued R903/78 virus is equivalent to the native V903/78 strain

The replication kinetics of the virus R903/78 recovered by reverse genetics was compared to the originally isolated native V903/78 virus [1,12]. It was previously determined that the great majority of virus (approximately 90%) was

DOI: 10.1002/jgm

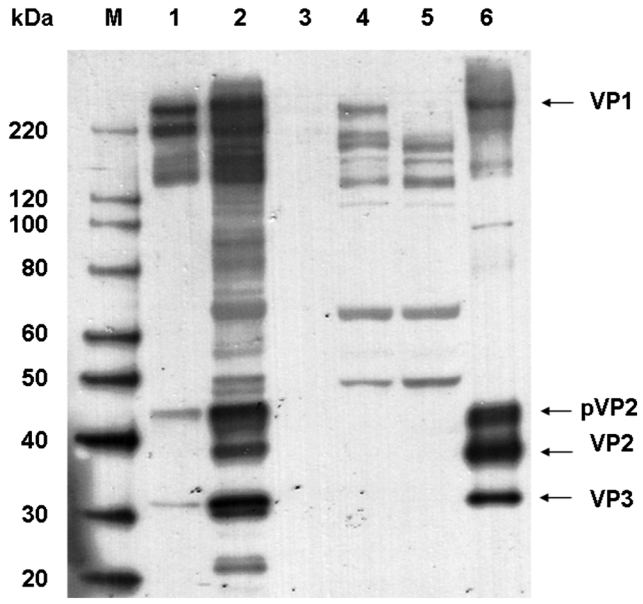

Figure 3. Immunoblot analysis of IBDV proteins synthesized in virus-infected Vero cells. Vero cells were co-transfected with pIBDV segment A and pIBDV segment B. At 5 days post-transfection, virus was harvested by three cycles of freeze–thaw. The lysed proteins were separated on 12.5% SDS-PAGE, blotted onto nitrocellulose and reacted with polyclonal anti-IBDV rabbit serum P2D78. Lane 1, 1 µl of Vero cell lysate (250 µl total) from 60 mm plate transfected with Superfect. Lane 2, 13 µl of Vero cell lysate (250 µl in total) from a 60-mm plate transfected with Superfect. Lane 3, 1 µl of Vero cell lysate (250 µl in total) from a 60-mm plate transfected with Dotap. Lane 4, 13 µl of Vero cell lysate (250 µl in total) from a 60-mm plate transfected with Dotap. Lane 5, 13 µl of Vero cell lysate (250 µl in total) from a 60-mm plate (nontransfected). Lane 6, 1.6×10^5 IU of the purified stock of IBDV serotype D78 (gift from Dr Vikram Vakharia, UMBC). The position of VP1, pVP2, VP2, VP3 and marker proteins (M) (kDa) is indicated.

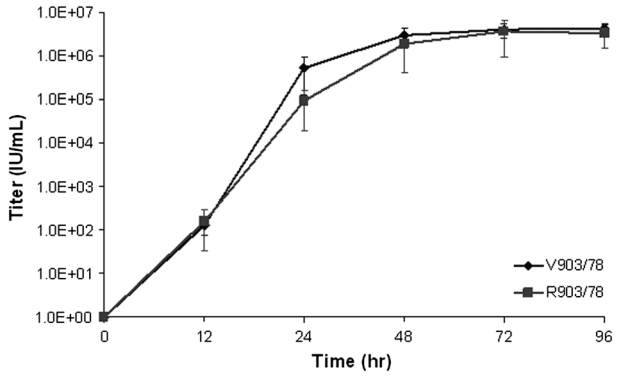

Figure 4. Growth kinetic comparisons of V903/78 and R903/78 viruses. Growth kinetics of viruses were analyzed in Vero cells. Vero cells were infected with the viruses at a MOI of 0.2 IU/cell. Virus yields were measured at the times indicated by the ICC assay on Vero cells. The symbols that represent the individual viruses are indicated adjacent to the growth curves. The results represent the averages of three independent experiments. Error bars indicate the SEM ($n = 3$). Student's t-test indicates no statistical difference between curves ($p = 0.62$).

secreted from cells and detected in the supernatant. The goal was to assess virus growth at maximum productivity at the lowest MOI. Therefore, the final virus titer was determined in a preliminary experiment at wide ranges of MOIs. It was found that, at a MOI of 0.2, the virus titer reached maximum at day 3 and higher MOIs did not increase virus yields. Although this result was counterintuitive from Poisson distribution of cell infection, it can be explained by rapid secretion of virus from cells. Therefore, virus stocks were appropriately diluted and Vero cells were infected with the viruses at a MOI of 0.2 for all growth curve experiments. Infected cell cultures were harvested at different time intervals and the titer of infectious virus present in the culture was determined by the ICC assay. The plot presented in Figure 4 represents the mean of triplicate independent experiments. The R903/78 and V903/78 viruses shared very similar overall patterns of replication, reaching virus titers of approximately 4.0×10^6 IU/ml after 4 days of infection. Although the replication of R903/78 virus was slightly delayed compared to V903/78 reaching a plateau, the delay was within an SD error range. Taken together, these data confirm equivalence of growth properties of the two viruses in cell culture on Vero cells (Student's t-test; $p = 0.62$). By contrast to some other IBDV serotypes [31], neither V903/78, nor R903/78 virus produced CPE on Vero cells and the great majority of virus was detected in the supernatant (data not shown).

The rescued R903/78 virus strain grows well on several human cell lines

Growth characteristics on other cell lines were compared to green monkey kidney Vero cells. The R903/78 virus titer increased in logarithmic fashion for 2 days, reaching virus titers of approximately 4.0×10^6 IU/ml after 3 days. This titer was maintained on day 4 as well without causing any observable CPE (Figure 4).

The growth kinetics was very similar in the human lung A549 cell line, although the final titer was somewhat lower than on Vero cells (Figure 5). In the human kidney cell line, HEK293, the titer increased very rapidly and reached 1.0×10^6 IU/ml after only 2 days. However, after that time point, the titer started to decline, resulting in a final titer of only 1.0×10^5 IU/ml at day 4. This decline coincided with a visible CPE and probable cell deterioration. It is possible that the adenovirus E1A and/or E1B sequences in this cell line caused interference with the IBDV virus, resulting in cell apoptosis. This hypothesis might be supported by evaluating other cell lines that were immortalized with adenovirus sequences such as the human

DOI: 10.1002/jgm

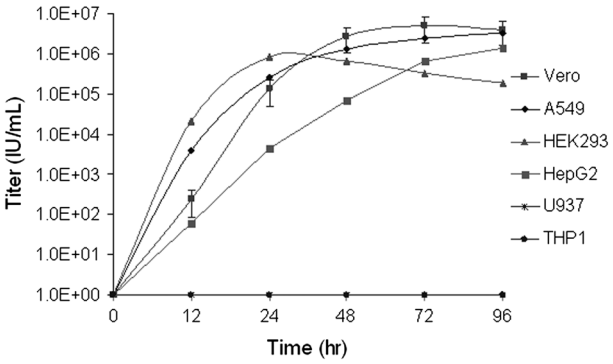

Figure 5. Growth kinetic of R903/78 on different cell lines. Growth kinetics of R903/78 was analyzed in A549, HEK293, HepG2, U937 and THP1 cells with Vero cell kinetics included from Figure 4 for comparison. Cells were infected with the R903/78 at a MOI of 0.2 IU/cell. Virus yields were measured at the times indicated by the ICC assay on Vero cells. The symbols that represent the individual cell lines are indicated adjacent to the growth curves. The results represent a single experiment. Analysis of variance between Vero, A549, HEK293 and HepG2 curves indicates that there might be a statistical difference between these curves ($p < 0.05$).

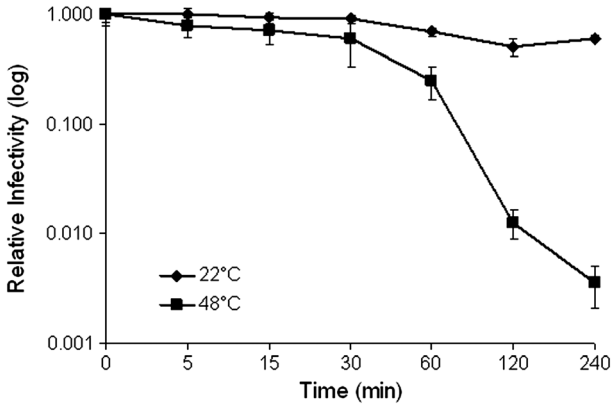

Figure 6. Thermostability evaluation of R903/78 virus. Duplicate aliquots of R903/78 were incubated at 22 °C and 48 °C for 0, 15, 30, 60, 120 and 240 min, and the titer of the virus was determined at the end of the assay. The plot represents the mean of two independent experiments. Error bars indicate the SD. Student's *t*-test indicates statistical significance between the two temperature curves ($p < 0.001$).

Per.C6 and 911 cell lines. In the human liver cell line, HepG2, titers increased in logarithmic manner for the 4-day duration of the experiment, reaching a final titer of 1.4×10^6 IU/ml at day 4. However, the slope of the Vero cell curve was much steeper than the HepG2 curve, which did not reach a plateau until day 4. Therefore, it is possible that HepG2 cells would have produced more virus if the experiment would have been extended (e.g. 6 days) (Figure 5). Previous experiments indicated that the IBDV replication was not associated with CPE or detrimental growth characteristics in HepG2 cells. This observation was confirmed in the present study as well. The U937 human lymphoma cell line and the THP1 human monocytic leukemia cell line did not provide any virus growth. These were the only cell lines grown in suspension culture, which may have affected virus propagation.

IBDV R903/78 shows extensive stability at a wide temperature range

To evaluate the thermostability of the R903/78 strain, the IBDV particles were analyzed in accelerated stability testing at room temperature (22 °C) and 48 °C [32,33]. The viral stock was diluted into PBS and incubated for various time periods. Residual infectivity was determined by the ICC assay on Vero cells and is expressed as a proportion of initial infectivity plotted on a logarithmic scale. The values shown are the mean of two separate determinations (Figure 6). Storage for 4 h at room temperature caused 40% loss of virus activity. A similar loss was observed at 48 °C in 30 min. Further incubation at 48 °C for 4 h caused a rapid drop of activity, resulting in approximately 0.4% of the original virus titer.

Previous experiments indicated that IBDV virus particles are very stable for long periods 4 °C (data not shown). IBDV thermostability appeared to be similar to the stability determined for the very stable wild type adenoviruses that can withstand short periods of temperature fluctuations. Therefore, long-term thermostability was evaluated under different temperature and formulation conditions. Initially, trehalose 5% (w/v) comprised of other formulation components was used, although some internally generated data suggested that higher concentrations of sugar might be beneficial for long-term storage. Also, trehalose is quite expensive. Therefore, the commonly used and much cheaper sugar sucrose was evaluated in parallel. The bulk harvest was purified using depth filtration and cross-flow filtration (CFF). During CFF, the concentrated virus suspension was washed with five discontinuous diafiltration steps and formulated with (A) 15% (w/v) sucrose or (B) 10% (w/v) sucrose and 5% (w/v) trehalose among other formulation components as described in the Materials and methods. Long-term storage was tested at 5 ± 3 °C and –70 °C. The stability study was carried out over a period of 6 months, with samples taken at 0, 1, 2, 3, 4, 5 and 6 months and evaluated for infectious titer with the ICC assay on Vero cells (Figure 7). Both formulations and storage temperatures indicated very good stability up to 6 months. At the 6-month time point, an apparent significant decrease of the titer is recognizable for the samples at 5 ± 3 °C, where both formulations at –70 °C are still very stable. However, formulation A at –70 °C shows a similar decrease in infectivity at 2 months, which can be explained by assay variability. Limited Student's *t*-test analysis would indicate that there is no statistical

DOI: 10.1002/jgm

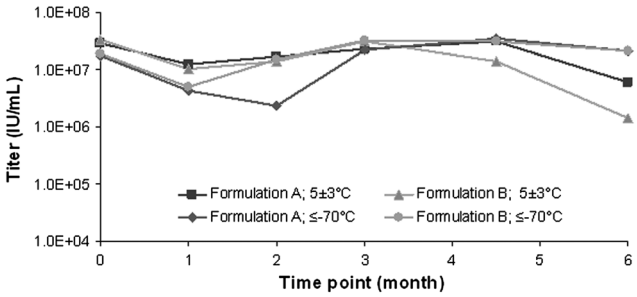

Figure 7. Long-term thermostability evaluation of R903/78 virus. Stability study of R903/78 on storage at 5 ± 3 °C and ≤ –70 °C in two different liquid formulations: (A) in 15% (w/v) sucrose or (B) 10% (w/v) sucrose and 5% (w/v) trehalose. Each formulation contained additional components as listed in the Materials and methods. Analysis of variance between the four curves indicates that there is no statistical difference between these curves ($p > 0.80$).

difference between these formulations ($p = 0.72$) and storage temperatures ($p = 0.66$). Therefore, it is crucial to follow-up the stability assays to confirm whether the drops for storage at 5 ± 3 °C are true and robust results. However, even if the stability at 5 ± 3 °C is not sufficient, alternative storage at ≤ –70 °C is possible.

IBDV R903/78 shows very extensive stability at low pH

To evaluate the pH stability of the R903/78 virus, the IBDV particles were tested over a wide range of pH conditions [34,35]. The pH stability was determined at 37 °C because it is assumed that the drug will be delivered orally and will pass through the stomach at body temperature. The viral stock was diluted into the appropriate buffer solution (VWR) at a ratio of 1:20 and incubated for 60 min at 37 °C assuming that this is a reasonable time to pass through the stomach. Residual infectivity was determined by the ICC assay on Vero cells and is expressed as a proportion of initial infectivity, plotted on a logarithmic scale (Figure 8). The values shown are the mean ± SD of two or three (pH 6 and 7) separate experiments. There was no significant change in virus titer from pH 6 to pH 8. At pH 10, the virus was rapidly inactivated because only 0.2% of the original virus activity was detected. At low pH, the virus was much more stable because, at pH 4, 60%, at pH 3, 16% and, at pH 2, 3% of the virus was still active. The virus stability was also determined at parallel incubations for 60 min in pH 6 and pH 7 solutions at 4 °C and 37 °C (data at 4 °C are not shown). The results of this experiment indicated that there was no significant change in virus titer under this condition as previously determined at 37 °C.

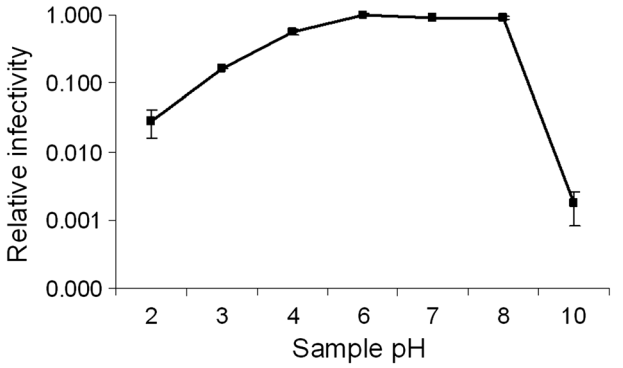

Figure 8. pH stability evaluation of R903/78 virus. Aliquots of R903/78 were incubated at the specified pH at 37 °C for 1 h. The aliquots were neutralized and the virus titer was determined at the end of the assay. The plot represents the percentage of residual infectivity values of the mean of the independent experiments at pH 6 and 7 and duplicate analysis at other points. Error bars indicate the SD. The amounts of residual infectivity values are compared with pH 6 to pH 8 (100%). At pH 10, 0.2%; pH 4, 60%; pH 3, 16% and pH 2, 3% of the virus was still active, respectively.

Multiple oral IBDV administrations in mice generate high levels of neutralizing antibodies

Neutralizing antibody response to oral and IV delivery of the IBDV clinical candidate vector R903/78 was measured with a virus neutralization test. Single administration of IBDV by the IV route generated the highest antibody response as expected (Figure 9). Both SO and MO delivery

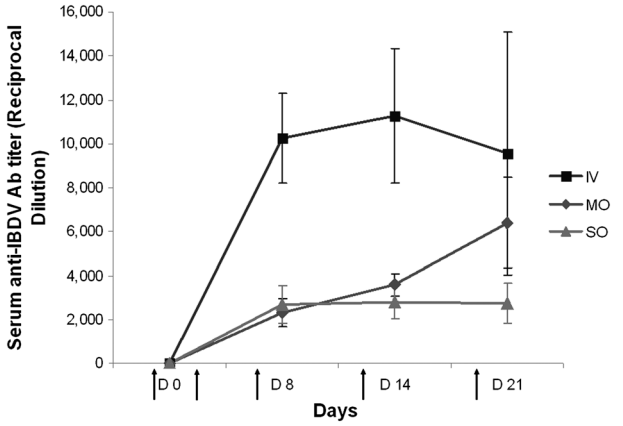

Figure 9. Kinetics of IBDV-specific neutralizing antibodies using end-point dilution data. Balb/C mice were immunized with IV, SO and MO delivery of 1.7×10^6 IU of R903/78 virus at day 0. MO mice also received the same amount of dose on days 3, 7, 13 and 20, respectively (indicated with arrows). At the indicated times, after administration, serum IBDV neutralizing antibodies were measured. Error bars indicate the SEM ($n = 4$). Student's *t*-test does not indicate statistical significance between MO and SO curves ($p = 0.35$), although a *Z*-test at day 21 shows a statistical difference ($p = 0.015$).

DOI: 10.1002/jgm

also elicited a rapid neutralizing antibody response in Balb/C mice. Surprisingly, it was difficult to distinguish between SO and MO responses within the error range. Statistical analysis between the MO and SO dosing curves indicated no statistical significance between curves ($p = 0.35$), although there is some indication for an increased titer at and beyond 21 days with MO administration ($p = 0.015$). Both end-point dilution (Figure 9) and 50% dilution curves (data not shown) are similar, although we expect the first one to be more precise. Antibody responses appear to peak between 14 and 21 days, as with other viruses; however, to determine more precisely the induced neutralizing antibody kinetics, it will be necessary to perform additional experiments. Initial observations indicated that MO delivery appeared to boost neutralizing antibody levels compared to SO delivery.

Effective repeat oral IBDV administration is possible in mice in the presence of high levels of IBDV neutralizing antibodies

To estimate the level of *in vivo* inhibition of IBDV virus delivery by neutralizing antibodies, the biodistribution of R903/78 was assessed in multiple organs using qRT-PCR. After MO delivery of the virus, tissue distribution of IBDV RNA was evaluated in blood, feces, liver, spleen, intestine, heart, lung, kidney and gonads using qRT-PCR [36]. The same quantity of 50 µl (1.7×10^6 IU) of R903/78 IBD virus was dosed in multiple oral deliveries. Within this project, a real-time qRT-PCR assay was developed for the specific and sensitive detection of the RNA of IBDV 903/78 strain. Based on the complete nucleotide sequence information (GenBank accession numbers JQ411012 and JQ411013), oligonucleotide primers and TaqMan probe were designed for the amplification of genetic regions of the A and B segments of IBDV. The primer-probe system was tested with extracted RNA from the V903/78 and R903/78 strains. Sensitivity of the assay was determined to detect approximately one to 10 genomic particles. All of the PCR results reported were performed with properly working positive standards and a negative control. All samples from untreated mice proved to be negative by qRT-PCR. A considerable amount of virus was detected in the organs subsequent to multiple oral deliveries. The results indicate a wide range of R903/78 tissue distribution with MO delivery that appears to produce a consistent presence of the virus in the liver, which is assumed to be the target tissue (Figure 10). All blood samples were negative, indicating fast clearance from the circulatory system.

The day 1 time point is equivalent to a single oral delivery. This time point indicates no detectable virus in the gonads and all other tissues showed borderline copy numbers, except the feces. The calculations indicate average data from four mice and, in every tissue, there were mice with undetectable virus copy numbers (except the feces). Therefore, the error in these values is large. The day 4 and day 8 time points also indicate low copy numbers, although virus RNA was detectable in all tissues tested, except in blood. The similar profile at day 4 and day 8 might indicate the effect of increasing amounts of neutralizing antibodies at the day 8 time point. There was a substantial increase in virus copy numbers in most organs at the day 14 time point. The highest amounts of virus RNA were detected in the liver, spleen, lung and kidney. At day 21, the level of virus copy numbers dropped one or more logs, except in the intestine, which is the result of a single outlier

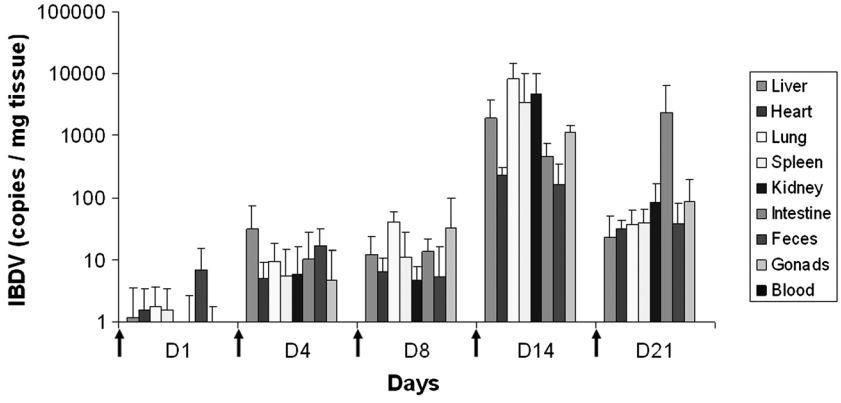

Figure 10. Tissue distribution of R903/78 virus following multiple oral administrations in mice. Virus was delivered in a 50-µl volume (1.7×10^6 IU) orally on days 0, 3, 7, 13 and 20 (indicated with arrows). Necropsy was performed on days 1, 4, 8, 14 and 21. Tissue RNA was quantified by quantitative real-time RT-PCR. Transduction efficiency is expressed as IBDV copy numbers per mg of tissue. Each bar represents the arithmetic mean of four independent experiments, except day 21 where one mouse died. Error bars indicate the SD ($n = 4$; $n = 3$ for day 21).

DOI: 10.1002/jgm

data point. Eliminating this data point would have caused a substantial drop compared to the day 14 time point consistent with other tissue distributions.

IBDV does not replicate in mice tissue

R903/78 IBD virus replication in mice cannot be confirmed definitively from the MO experiments. The almost identical level of virus copy numbers at the day 4 and day 8 time points indicates viral stability rather than evidence of viral replication because the amount of viral RNA does not appear to increase throughout the time period. The other possibility is the effect of increasing IBDV specific antibodies, as discussed above. However, the substantial increase in viral specific RNA at the day 14 time point could indicate viral replication regardless of the presence of neutralizing antibodies. Moreover, the substantial decrease of viral RNA at the day 21 time point coincides with the increase in neutralizing antibodies against the virus (Figure 9).

To clarify these issues, mice were dosed with a single delivery of R903/78 IBD virus SO and IV. Virus genomes were quantified at days 4, 8, 14 and 21 after delivery to animals. After SO delivery, no virus genomes were detectable in any of the treated mice at any time points in the liver (data not shown). These data were in contrast to MO delivery where low levels (but detectable) of virus genome were present in most tissues at day 1 and a large increase of viral genome was observed at day 4 (Figure 10). These data indicate viral stability and genome accumulation under the multiple dosing scenario and not viral replication. The view that IBDV does not replicate in mice liver is further reinforced by the single-dose IV delivery data (Figure 11). The large amounts of viral genome accumulation at day 4 and its rapid decrease would be difficult to explain by anti-viral immunity if there was substantial viral replication.

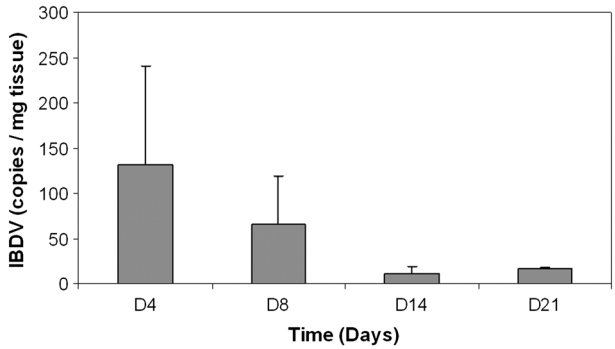

Figure 11. Tissue presence of R903/78 virus following single IV administrations in mice. Virus was delivered in a 50-µl volume (1.7×10^6 IU) IV on days 0. Necropsy was performed on days 4, 8, 14 and 21. Liver RNA was quantified by quantitative real-time RT-PCR. Transduction efficiency is expressed as IBDV copy numbers per mg of tissue. Each bar represents the arithmetic mean of four independent experiments, except day 21 where one mouse died. Error bars indicate the SEM ($n = 4$; $n = 3$ for day 21).

Discussion

It is close to 20 years since the first IBDV virus was created using reverse genetics [10–12]. This great achievement was followed by improvement on the process a decade later [11,37,38]. The ability to rescue infectious viruses from cloned cDNAs has been well established already and allowed systematic studies of viral characteristics. Several laboratories successfully incorporated foreign epitopes at different locations into the viral genome in the hope of developing vaccines for multiple disease targets [12,39,40]. Attempts were also made to incorporate exogenous genes into the IBDV genome but, until now, these experiments did not succeed [12]. This is probably a result of the restricted packaging size of the dsRNA genome. In any event, reverse genetics allowed us to clone the IBDV V903/78 serotype genome and recreate it as the artificial virus R903/78. The two viruses have identical genomes, although the later can be manufactured without any concerns of labor intensive re-plaquing in case of the appearance of contaminant quasispecies [41] or interfering small plaque mutant viruses [42], which is especially important if the virus is to be used in human therapy [20]. Consequently, we investigated several basic characteristics of the R903/78 virus and so this agent might be used in a planned human clinical trial to eliminate HBV and HCV viral loads employing superinfection therapy [20].

Phylogenic analysis indicated that V903/78 is closely related to the D78 vaccine strain. Although, the 5-nucleotides difference in the coding region of segment A resulted in amino acid changes in VP5, VP2 and VP4, these changes did not appear to influence cell tropism and virulence. Changes in the coding region of segment B did not result in amino acid changes. It has been deduced that IBDV 5'- and 3'-noncoding regions are very important [5]. Both segment A and B had three differences in the noncoding regions between V903/78 and D78. A 3-nucleotides deletion in segment A was present just proximal to the important 3'-untranslated region stem-loop [43]. However, chimeric viruses constructed by exchanging noncoding regions between the two virus strains [44] did not indicate significant changes in growth patterns (data not shown).

The evaluation of IBDV R903/78 virus growth characteristics is an important question from both safety and manufacturing perspectives. In the present study, the

DOI: 10.1002/jgm

virus growth properties were evaluated in a single-step growth curve on several cell lines. At the present time, the virus is manufactured on green monkey kidney Vero cells and therefore all other growth characteristics were compared with this cell line.

IBDV vaccine strains grow well on several avian cell lines such as CEF and DF-1 [1,45]. IBDV strains have also been shown to grow well on RK13 rabbit kidney cells without causing any CPE and also grow to high titer on BHK21 baby hamster kidney cells where no CPE is produced [46]. In addition, primate cells have also been evaluated [47] and IBDV animal vaccines are mostly produced on Vero cells [1]. However, we found only two human cell lines, HEK293 [12] and HEK293T [48], that were assessed for IBDV growth. Apparently, we have observed very similar kinetics to previous studies on HEK293 cells where the titer reached a peak on day 2 and then declined, possibly indicating deterioration of the cells. The ability of IBDV to propagate in HEK293 and primate cells [49] suggests that IBDV might be capable of limited replication in mammals, including in humans. Additionally, replication of IBDV in human cells will establish its potential to be used as therapeutics for human diseases.

The clinical target of the IBDV-superinfection therapy for hepatitis is the liver. Therefore, it was important to show that R903/78 was propagating on HepG2 cells without any detrimental effects. Although with slower kinetics compared to Vero cells, there was substantial viral replication on this cell line without any visible CPE or sign of detrimental effect to the cells (data not shown). Therefore, this human cell line could be used for *in vitro* model studies of viral interference between IBDV and other liver specific viruses. A549 cells are used to produce replication efficient adenovirus for clinical trials [50]. The similar growth pattern in this cell line compared to Vero cells provides the possibility for manufacturing R903/78 on A549 cells. IBDV is a lymphothropic virus and it was surprising that it did not propagate on human lymphoma and monocytic leukemia cell lines. At this point, it is not known whether these cell lines were infected at all or viral replication was repressed for some other reason. A likely reason is these cells do not have the proper receptors for IBDV infection. Further studies should be able to distinguish between these propositions.

IBDV has been described as a very stable virus [46,51]; however, the amount of data supporting this statement are quite scarce. Therefore, we have evaluated accelerated and long-term stability studies in different temperatures with purified virus substance without serum to stabilize the capsids. The accelerated temperatures stability study indicated that, at 48 °C, very little infectious virus survived. This is contrast to previous studies where, at 55 °C after 3 h of incubation, little loss of activity was observed [46]. This contradiction could be explained by the formulation. The liquid formulation in the present study was derived from the serum and animal free composition developed for adenovirus gene therapy products [52]. Furthermore, in contrast to adenovirus, IBDV is much more stable at low than at high pH. Therefore, in the future, different formulations will be evaluated and a buffer with a more neutral pK_a value, such as PBS, will be chosen. Despite the short-term stability results, the long-term temperature study indicated excellent stability at both 5 °C and –70 °C for 6 months. Tris buffer has a large negative temperature coefficient and the pH 7.8 buffer measured at room temperature could have been close to pH 8.4 at 5 °C, somewhat reducing stability. The sensitivity of R903/78 to extremely low and especially high pH ranges might also have been exaggerated by the use of the particular formulation. In any event, the generated stability data for the liquid formulation stored at 5 °C is very promising. The IBDV pH stability is much better than the similarly heat stable adenovirus serotype 5 that is inactivated at pH 5. However, it appears to be less stable than some enteroviruses such as HAV that drop in activity by only approximately one log after 1 h of incubation at 38 °C at pH 1 [53]. The significant loss of R903/78 stability at pH2 (3% of infectivity, as shown in Figure 8) predicts poor *in vivo* recovery of our drug candidate strain after oral administration. Therefore, the aim is to improve R903/78 strain stability in stomach acids by administering our therapeutic drug candidate in enteric coated capsules.

Evaluation of neutralizing antibody generation by IBDV is essential for the estimation of efficacy of multiple oral deliveries planed for the human clinical trials [20]. Serological assays for the assessment of different virus neutralizing antibodies have been previously developed for many viruses [54,55]. The amount of neutralizing antibody generated by multiple oral delivery of IBDV is critical for the assessment of efficiency in planned clinical trials [20]. Most viruses cannot be delivered multiple times because the immune responses to the virus capsids prevent serial infections. In gene therapy applications, effective repeat administration of adenovirus vectors after intranasal or IV delivery is hindered by a strong neutralizing antibody response to the vector. However, intramuscular administration of adenovirus vectors elicited a neutralizing antibody response that peaked between 14 and 21 days after infection, although effective repeat intramuscular administration of adenovirus vectors was not hindered by the presence of neutralizing antibodies in the serum [56].

IBDV is not pathogenic to mammals, although mice might be potential carriers of the virus [57]. Also, it has been proposed that IBDV could be transmitted through dog hosts [58]. In the present study, we used Balb/C mice to assess immune responses to the virus and the presence

DOI: 10.1002/jgm

of viral genome in different tissues. Based on clinical experience, we assumed that, by using large virus doses continuously for a longer period of time, IBDV infection will be detected despite the presence of anti-IBDV antibodies. Moreover, we assumed that oral dosing of a stable virus such as IBDV will survive passage through the acidic environment of the stomach and will elicit mucosal immune responses in the gut. Similar to a previous human clinical trial [14], multiple oral dosing (MO) was carried out in mice. We also dosed mice with SO and with IV injection as a control. Not surprisingly, IV injected mice responded by the production of large amounts of antibodies. Also as expected, SO administration elicited a rapid neutralizing antibody response. MO administration boosted a response somewhat comparable to SO at day 21 after dosing, although this did not reach a plateau at this point. The amount of neutralizing antibody in the blood did not prevent virus delivery to the tissues. In the present study, we did not explore the means of virus delivery to tissues, although it is possible that IBDV is picked up by gut macrophages or other lymphoid cells and then dispersed throughout the body [59,60].

Form the MO delivery experiments, we cannot decisively confirm whether IBDV replicates in mouse tissues or only accumulates through multiple deliveries. Although there was a very large increase in viral RNA in all different tissues at the day 14 time point, this could have been the consequence of the newly delivered virus at day 13. The diminished amounts of viral genomes detected at day 21 coincide with increasing amounts of neutralizing antibodies.

The undetectable levels of viral genome in SO administration at day 4 and all other time points indicate viral stability rather than viral replication. This observation is reinforced by the single IV administration data showing diminishing genome levels throughout the time course of the experiment.

A very important issue, the *in vivo* neutralizing effects of the R903/78 antibodies, is still incompletely answered by our experiments shown in Figures 9 and 10 because the confounding effects of (i) virus stability; (ii) virus biodistribution/retention in different organs; (iii) virus replication in different organs and (iv) the influence of neutralizing antibodies could not be adequately dissected from each other. Accordingly, we aim to determine the amounts of free virus in the organs at different time point after a single dosing experiment simultaneously in immune competent and immune deficient mice, respectively. In this way, putative virus replication can be separated from the inhibitory effect of virus neutralization.

Nevertheless, clinical experience demonstrated that the IBDV superinfection therapy was effective in several decompensated chronic hepatitis patients, showing striking clinical improvement without side effects when large doses of the viral preparation were administered continuously over a long period to ensure maintenance of 'artificial viremia' by IBDV, which is not known to infect human beings naturally [14,20]. This is consistent with the observation that repeated intranasal or intravenous administration of Newcastle disease virus remained effective in cancer patients despite the presence of neutralizing antibodies [61].

We are currently completing a chronic GLP toxicology study with the R903/78 drug candidate in which long-term (12 weeks) administration of the planned human clinical study was modelled. One of the objectives of the study was to determine the true peak of the antibody response. It is, however, still not clear how the virus in tissues and antibodies in the circulation reach equilibrium during long-term continuing oral dosing, and this remains to be investigated in animals that have received passive transfer of 'neutralizing antibodies'.

In all of the *in vivo* experiments, no pathology or unusual behavior of mice was observed. Although mice [57], rats [62] and dogs [58] were proposed as possible carriers of IBDV, this virus was not shown to be a pathogen in mice and its ability to spread in mammals is probably relatively low. Consistent with this, in our experiments, the Vero cell line adapted, attenuated R903/78 IBD virus appears to be safe for mice. The R903/78 virus was detected in all organs tested, except for blood, even at day 21 after the initiation of MO administration. This indicates that the virus is stably retained. SO and IV administration suggested that IBDV does not replicate in the liver, despite the fact that it does replicate in the HepG2 human liver cell line. Because IBDV replication does not go through a DNA intermediate, it is unlikely that its genome material is transmitted to subsequent generations through the gonads, alleviating some safety related concerns. These biodistribution data appear to concur with previous observations indicating that multiple and long-term oral dosing is needed for any clinical benefit in human disease [14].

Acknowledgements

We thank Aleksandr Krendelshchikov for providing technical assistance and Gergely Németh for continued support of this project. We also thank Dr Vikram Vakharia of UMBC for providing the IBDV strain D78 and the anti-IBDV rabbit serum P2D78. The project was supported in part by the EUROSTARS-HU-07-1-2011-0006 grant with the project acronym: 'SITVH' in Hungary and EUROSTARS/BMBF 01QE1138A grant with the project acronym 'E!6559 Superinfection' in Germany. The authors declare that Imre Kovesdi and Tibor Bakács are equity holders in HepC, Ltd.

References

1. Kibenge FS, Dhillon AS, Russell RG. Growth of serotypes I and II and variant strains of infectious bursal disease virus in Vero cells. *Avian Dis* 1988; **32**: 298–303.
2. Berg TP. Acute infectious bursal disease in poultry: a review. *Avian Pathol* 2000; **29**: 175–194.
3. Pedersden KA, Sadasiv EC, Chang PW, *et al.* Detection of antibody to avian viruses in human populations. *Epidemiol Infect* 1990; **104**: 519–525.
4. Dobos P, Hill BJ, Hallett R, *et al.* Biophysical and biochemical characterization of five animal viruses with bisegmented double-stranded RNA genomes. *J Virol* 1979; **32**: 593–605.
5. Mundt E, Muller H. Complete nucleotide sequences of 5'- and 3'-noncoding regions of both genome segments of different strains of infectious bursal disease virus. *Virology* 1995; **209**: 10–18.
6. Pan J, Vakharia VN, Tao YJ. The structure of a birnavirus polymerase reveals a distinct active site topology. *Proc Natl Acad Sci U S A* 2007; **104**: 7385–7390.
7. von Einem UI, Gorbalenya AE, Schirrmeier H, *et al.* VP1 of infectious bursal disease virus is an RNA-dependent RNA polymerase. *J Gen Virol* 2004; **85**: 2221–2229.
8. Mundt E. Tissue culture infectivity of different strains of infectious bursal disease virus is determined by distinct amino acids in VP2. *J Gen Virol* 1999; **80**: 2067–2076.
9. Conzelmann KK. Nonsegmented negative-strand RNA viruses: genetics and manipulation of viral genomes. *Annu Rev Genet* 1998; **32**: 123–162.
10. Mundt E, Vakharia VN. Synthetic transcripts of double-stranded birnavirus genome are infectious. *Proc Natl Acad Sci U S A* 1996; **93**: 11131–11136.
11. Ben Abdeljelil N, Khabouchi N, Mardassi H. Efficient rescue of infectious bursal disease virus using a simplified RNA polymerase II-based reverse genetics strategy. *Arch Virol* 2008; **153**: 1131–1137.
12. Upadhyay C, Ammayappan A, Patel D, *et al.* Recombinant infectious bursal disease virus carrying hepatitis C virus epitopes. *J Virol* 2011; **85**: 1408–1414.
13. Bakacs T, Mehrishi JN. Intentional coinfection of patients with HCV infection using avian infection bursal disease virus. *Hepatology* 2002; **36**: 255.
14. Csatary LK, Schnabel R, Bakacs T. Successful treatment of decompensated chronic viral hepatitis by bursal disease virus vaccine. *Anticancer Res* 1999; **19**: 629–633.
15. Guidotti LG, Borrow P, Hobbs MV, *et al.* Viral cross talk: intracellular inactivation of the hepatitis B virus during an unrelated viral infection of the liver. *Proc Natl Acad Sci U S A* 1996; **93**: 4589–4594.
16. Davis GL, Hoofnagle JH, Waggoner JG. Acute type A hepatitis during chronic hepatitis B virus infection: association of depressed hepatitis B virus replication with appearance of endogenous alpha interferon. *J Med Virol* 1984; **14**: 141–147.
17. Csatary LK, Kasza L, Massey RJ. Interference between human hepatitis A virus and an attenuated apathogenic avian virus. *Acta Microbiol Hung* 1984; **31**: 153–158.
18. Koike K, Yasuda K, Yotsuyanagi H, *et al.* Dominant replication of either virus in dual infection with hepatitis viruses B and C. *J Med Virol* 1995; **45**: 236–239.
19. Fan X, Lang DM, Xu Y, *et al.* Liver transplantation with hepatitis C virus-infected graft: interaction between donor and recipient viral strains. *Hepatology* 2003; **38**: 25–33.
20. Bakacs T, Mehrishi JN. Examination of the value of treatment of decompensated viral hepatitis patients by intentionally coinfecting them with an apathogenic IBDV and using the lessons learnt to seriously consider treating patients infected with HIV using the apathogenic hepatitis G virus. *Vaccine* 2004; **23**: 3–13.
21. Csatary LK, Telegdy L, Gergely P, *et al.* Preliminary report of a controlled trial of MTH-68/B virus vaccine treatment in acute B and C hepatitis: a phase II study. *Anticancer Res* 1998; **18**: 1279–1282.
22. Lukert PD, Saif YM. Infectious bursal disease. In *Diseases of poultry*, Calnek BW (ed). Wiley: Chichester, 1997; 721–738.
23. Eterradossi N. Infectious bursal disease (Gumboro disease). *OIE the World Organization for Animal Health* 2008; 549–565. http://www.oie.int/international-standard-setting/terrestrial-manual/access-online/
24. Da Costa B, Soignier S, Chevalier C, *et al.* Blotched snakehead virus is a new aquatic birnavirus that is slightly more related to avibirnavirus than to aquabirnavirus. *J Virol* 2003; **77**: 719–725.
25. Ammayappan A, Vakharia VN. Molecular characterization of the Great Lakes viral haemorrhagic septicemia virus (VHSV) isolate from USA. *Virol J* 2009; **6**: 171.
26. Van de Peer Y, De Wachter R. TREECON for Windows: a software package for the construction and drawing of evolutionary trees for the Microsoft Windows environment. *Comput Appl Biosci* 1994; **10**: 569–570.
27. Bayliss CD, Spies U, Shaw K, *et al.* A comparison of the sequences of segment A of four infectious bursal disease virus strains and identification of a variable region in VP2. *J Gen Virol* 1990; **71**: 1303–1312.
28. Jackwood DJ, Sreedevi B, LeFever LJ, *et al.* Studies on naturally occurring infectious bursal disease viruses suggest that a single amino acid substitution at position 253 in VP2 increases pathogenicity. *Virology* 2008; **377**: 110–116.
29. Brandt M, Yao K, Liu M, *et al.* Molecular determinants of virulence, cell tropism, and pathogenic phenotype of infectious bursal disease virus. *J Virol* 2001; **75**: 11974–11982.
30. van Loon AA, de Haas N, Zeyda I, *et al.* Alteration of amino acids in VP2 of very virulent infectious bursal disease virus results in tissue culture adaptation and attenuation in chickens. *J Gen Virol* 2002; **83**: 121–129.
31. Ahasan MM, Hossain KM, Islam MR. Adaptation of infectious bursal diseas virus (IBDV) on Vero cell line. *Online J Biol Sci* 2002; **2**: 633–635.
32. Caravokyri C, Leppard KN. Constitutive episomal expression of polypeptide IX (pIX) in a 293-based cell line complements the deficiency of pIX mutant adenovirus type 5. *J Virol* 1995; **69**: 6627–6633.
33. Smith AC, Poulin KL, Parks RJ. DNA genome size affects the stability of the adenovirus virion. *J Virol* 2009; **83**: 2025–2028.
34. Hale JM. A study of the pH stability of vaccinia virus. *Yale J Biol Med* 1942; **15**: 241–258.
35. Scholtissek C. Stability of infectious influenza A viruses to treatment at low pH and heating. *Arch Virol* 1985; **85**: 1–11.
36. Xu XX, Shui X, Chen ZH, *et al.* Development and application of a real-time PCR method for pharmacokinetic and biodistribution studies of recombinant adenovirus. *Mol Biotechnol* 2009; **43**: 130–137.
37. Ben Abdeljelil N, Delmas B, Mardassi H. Replication and packaging of an infectious bursal disease virus segment A-derived minigenome. *Virus Res* 2008; **136**: 146–151.
38. Boot HJ, ter Huurne AA, Peeters BP, *et al.* Efficient rescue of infectious bursal disease virus from cloned cDNA: evidence for involvement of the 3'-terminal sequence in genome replication. *Virology* 1999; **265**: 330–341.
39. Li K, Gao L, Gao H, *et al.* Recombinant infectious bursal disease virus expressing Newcastle disease virus (NDV) neutralizing epitope confers partial protection against virulent NDV challenge in chickens. *Antiviral Res* 2014; **101**: 1–11.
40. Mosley YY, Wu CC, Lin TL. An influenza A virus haemagglutinin (HA) epitope inserted in and expressed from several loci of the infectious bursal disease virus genome induces HA-specific antibodies. *Arch Virol* 2014; **159**: 2033–2041.
41. Jackwood DJ, Sommer SE. Identification of infectious bursal disease virus quasispecies in commercial vaccines and field isolates of this double-stranded RNA virus. *Virology* 2002; **304**: 105–113.
42. Muller H, Lange H, Becht H. Formation, characterization and interfering capacity

of a small plaque mutant and of incomplete virus particles of infectious bursal disease virus. *Virus Res* 1986; **4**: 297–309.
43. Boot HJ, Pritz-Verschuren SB. Modifications of the 3′-UTR stem-loop of infectious bursal disease virus are allowed without influencing replication or virulence. *Nucleic Acids Res* 2004; **32**: 211–222.
44. Boot HJ, ter Huurne AA, Vastenhouw SA, *et al.* Rescue of infectious bursal disease virus from mosaic full-length clones composed of serotype I and II cDNA. *Arch Virol* 2001; **146**: 1991–2007.
45. Rekha K, Sivasubramanian C, Chung IM, *et al.* Growth and replication of infectious bursal disease virus in the DF-1 cell line and chicken embryo fibroblasts. *Biomed Res Int* 2014; **2014**: 494835.
46. Petek M, D'Aprile PN, Cancellotti F. Biological and physico-chemical properties of the infectious bursal disease virus (IBDV). *Avian Pathol* 1973; **2**: 135–152.
47. Dahling DR, Wright BA. Optimization of the BGM cell line culture and viral assay procedures for monitoring viruses in the environment. *Appl Environ Microbiol* 1986; **51**: 790–812.
48. Li Z, Wang Y, Li X, *et al.* Critical roles of glucocorticoid-induced leucine zipper in infectious bursal disease virus (IBDV)-induced suppression of type I Interferon expression and enhancement of IBDV growth in host cells via interaction with VP4. *J Virol* 2013; **87**: 1221–1231.
49. Jackwood DH, Saif YM, Hughes JH. Replication of infectious bursal disease virus in continuous cell lines. *Avian Dis* 1987; **31**: 370–375.
50. Kimball KJ, Preuss MA, Barnes MN, *et al.* A phase I study of a tropism-modified conditionally replicative adenovirus for recurrent malignant gynecologic diseases. *Clin Cancer Res* 2010; **16**: 5277–5287.
51. Benton WJ, Cover MS, Rosenberger JK, *et al.* Physicochemical properties of the infectious bursal agent (IBA). *Avian Dis* 1967; **11**: 438–445.
52. Rasmussen H, Rasmussen C, Lempicki M, *et al.* TNFerade Biologic: preclinical toxicology of a novel adenovector with a radiation-inducible promoter, carrying the human tumour necrosis factor alpha gene. *Cancer Gene Ther* 2002; **9**: 951–957.
53. Scholz E, Heinricy U, Flehmig B. Acid stability of hepatitis A virus. *J Gen Virol* 1989; **70**: 2481–2485.
54. Golding SM, Hedger RS, Talbot P. Radial immuno-diffusion and serum-neutralization techniques for the assay of antibodies to swine vesicular disease. *Res Vet Sci* 1976; **20**: 142–147.
55. Loeffen W, Quak S, de Boer-Luijtze E, *et al.* Development of a virus neutralization test to detect antibodies against Schmallenberg virus and serological results in suspect and infected herds. *Acta Vet Scand* 2012; **54**: 44.
56. Chen P, Kovesdi I, Bruder JT. Effective repeat administration with adenovirus vectors to the muscle. *Gene Ther* 2000; **7**: 587–595.
57. Park MJ, Park JH, Kwon HM. Mice as potential carriers of infectious bursal disease virus in chickens. *Vet J* 2010; **183**: 352–354.
58. Pages-Mante A, Torrents D, Maldonado J, *et al.* Dogs as potential carriers of infectious bursal disease virus. *Avian Pathol* 2004; **33**: 205–209.
59. Delgui L, Gonzalez D, Rodriguez JF. Infectious bursal disease virus persistently infects bursal B-lymphoid DT40 cells. *J Gen Virol* 2009; **90**: 1148–1152.
60. Khatri M, Sharma JM. Modulation of macrophages by infectious bursal disease virus. *Cytogenet Genome Res* 2007; **117**: 388–393.
61. Csatary LK, Moss RW, Beuth J, *et al.* Beneficial treatment of patients with advanced cancer using a Newcastle disease virus vaccine (MTH-68/H). *Anticancer Res* 1999; **19**: 635–638.
62. Okoye JOA, Uche UE. Serological evidence of infectious bursal disease virus infectious in wild rats. *Acta Vet Brno* 1986; **55**: 207–209.